Understanding the Properties of the Coagel and Gel Phases: A ^{2}H and ^{13}C NMR Study of Amphiphilic Ascorbic Acid Derivatives

Silvia Borsacchi,[†] Moira Ambrosi,[‡] Pierandrea Lo Nostro,[‡] and Marco Geppi*[,†]

Department of Chemistry and Industrial Chemistry, University of Pisa, via Risorgimento 35, 56126 Pisa, Italy, and Department of Chemistry and CSGI, University of Florence, 50019 Sesto Fiorentino, Firenze, Italy

Received: August 4, 2010; Revised Manuscript Received: October 19, 2010

The coagel and gel phases formed by the D and L diastereoisomers of ascorbyl-dodecanoate (ASC12) in deuterated water were studied through solid-state NMR techniques. In particular, the dynamic properties of water and surfactant chains were investigated by ^{2}H and ^{13}C NMR static spectra, respectively. Two fractions of water with very different dynamics were found in the coagel phases, one solidlike and one liquidlike, assigned to water strongly bound to the surfactant polar heads and bulk water, respectively. Only one kind of "intermediate" water was instead detected in the gel phase suggesting that the merging of the two types of water in the interlayers between the surfactant lamellae occurs at the coagel-to-gel transition. Moreover, the surfactant chains, very rigid in the coagel phase, give rise to fast trans−gauche interconformational jumps in the gel phase, where almost isotropic reorientations of the whole aggregates also occur. A different dynamic behavior was found for the two diastereoisomers in particular for what concerns the surfactant molecules in the gel phase and the water molecules in the coagel presumably ascribable to different inter- and intramolecular interactions that involve the polar heads.

Introduction

Because of their amphiphilic nature, surfactants form a variety of self-assembled nanostructures in water. Their size and shape and the physicochemical equilibrium properties of these aggregates depend on their composition, that is, on the charge and the hydrogen-bonding capacity of the head groups, on the length of the hydrophobic segments, as well as on temperature, concentration, and presence of electrolytes or neutral cosolutes.[1]

The stability and properties of these aggregates are determined by noncovalent interactions that include van der Waals, hydrophobic, hydration, dipolar, and electrostatic forces. The same forces are at play in all biologically relevant systems (biomembranes, nucleic acid complexes, antigen−antibody, enzyme−substrate adducts, etc.). Therefore, self-assemblies produced by relatively simple building blocks, such as surfactants, are an extremely useful tool to understand the processes, such as molecular recognition, that control the functions and activities of higher hierarchical structures. The self-assembly properties of 6-*O*-ascorbyl-alkanoates in water are particularly interesting because these surfactants bear an ascorbic acid residue as polar head group. This moiety possesses a quite rigid lactone ring, a redox active group, and three hydroxyl groups that are available for hydrogen bonding and carries two stereogenic centers in positions 4 and 5. Such structural features determine the formation of nano-self-assemblies.[2]

The self-assembly properties of ascorbyl-alkanoates in water have been studied extensively by means of conductivity, differential scanning calorimetry (DSC), surface tension, small-angle X-ray scattering (SAXS), small-angle neutron scattering (SANS), cryo-transmission electron microscopy (cryo-TEM), and X-ray diffraction (XRD) experiments. In previous papers, we have investigated the behavior of single-chain L-ascorbic acid esters (L-ASC*n*, where *n* refers to the number of carbons in the side chain) in water with *n* ranging between 8 and 18.[3−13] We have also studied the effect of pH, addition of salts, sugars, urea, glycerol, and poly(ethylene glycol) PEG polymers.[14,15] More recently, we studied the self-assembly of a bolaamphiphile that carries two L-ascorbic acid moieties as head groups[2] and of a double-chained derivative.[16]

The effect of the stereochemical features of the hydrophilic head groups was assessed by studying the esters obtained from the diastereoisomeric D-isoascorbic acid (D-ASC*n*), where the C5 stereogenic center has the opposite configuration than that in L-ascorbic acid.[17] The results show that the physicochemical properties of L- and D-ASC*n* are significantly different in the solid and in the dispersed states.[18] In particular, the hydration of the head groups changes because of the different set of hydrogen bonds. In fact, L-ascorbic acid groups can form several intermolecular bonds, while intramolecular interactions prevail in the D-isoascorbic units. Such a structural feature determines also the thermal behavior of their mixtures with the formation of eutectic points and equimolar molecular compounds.[18]

Once these surfactants are dispersed in water, they can form two different stable phases depending on temperature. At relatively low temperature, and at a surfactant concentration larger than 1−2% w/w, L-ASC*n* and D-ASC*n* form "coagels" in water. Upon heating, the coagel structure collapses and transforms into a clear liquid micellar dispersion for ASC*n* with $n = 8$ and 10, while for larger *n* a "gel" is formed. The term gel was introduced and was adopted in the literature because of the appearance of a translucent, highly viscous phase in the sample. The temperature at which the coagel turns into the micellar or the gel state was detected through conductivity and DSC and is strictly related to the number of carbons in the lipophilic block. The transition temperature does not significantly change when the surfactant concentration ranges between 5% and 50% w/w. The coagel state is usually depicted as a tight

* To whom correspondence should be addressed. E-mail: mg@dcci.unipi.it. Fax: +39-0502219260. Phone: +39-0502219289.
[†] University of Pisa.
[‡] University of Florence.

10.1021/jp107324e
Published on Web 11/15/2010

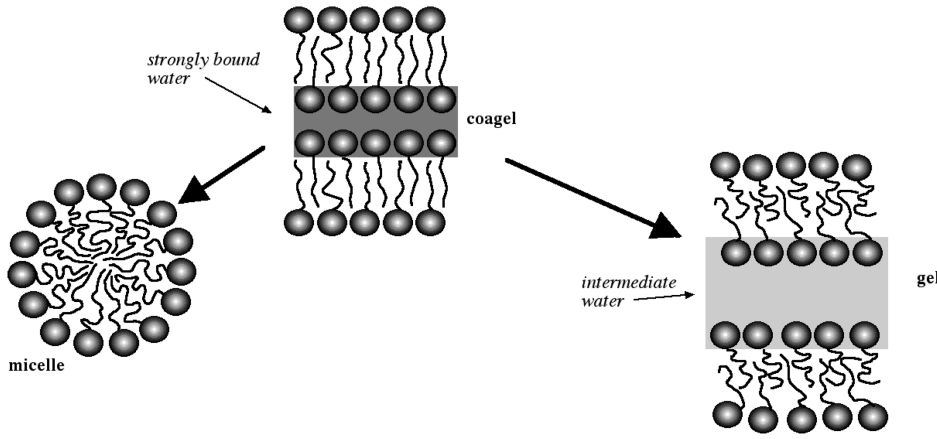

Figure 1. Schematic picture of a micellar aggregate and coagel and gel phases of ASC*n*/water.

lamellar hydrated and semicrystalline phase, where the aliphatic tails are arranged in compact layers with interdigitated chains and a low degree of tilting. In the coagel, a thin layer (about 1 nm resulting, for instance, from the difference of *d*-spacing values of about 38.6 Å[14] and 28 Å[17] for coagel and anhydrous phases of ASC12) of strongly bound water molecules is confined between the hydrophilic regions of two adjacent lamellae. Bulk water is also present in the sample at the equilibrium. Optical microscopy under crossed polarizers and environmental scanning electron microscope (ESEM) micrographs show the presence of extended highly oriented structures, similar to a house of cards, like those found in smectic liquid crystals.[14] As the temperature is increased above the transition point, the bulk free water disappears, and in the gel state the surfactant lamellar layers are supposed to be separated by a much larger water pool. This water is usually referred to as intermediate water (see Figure 1). Such a scheme parallels that proposed by Kodama and Seki for aqueous dispersions of quaternary ammonium single chained cationic amphiphiles.[19] However, this model has been criticized by Laughlin and co-workers[20−22] who proposed the simpler dehydration of the surfactant head groups upon heating as the main mechanism of the observed phase transition. According to Kodama and Seki, the enthalpy change that follows the coagel-to-gel transition can be divided into three different contributions: ΔH_{el} that accounts for the release of the counterion from the head group (in our case a H^+ ion), ΔH_{hydr} that reflects the hydration of the hydrophilic groups, and ΔH_{chain} that is the uptake of heat related to the partial melting of the lipophilic chains that in the less ordered gel state possess a higher lateral freedom of motion. ΔH_{el} and ΔH_{chain} are endothermic contributions, while ΔH_{hydr} is exothermic. The amount of strongly bound water can be conveniently obtained by means of DSC experiments by comparing the total stoichiometric mass of water added to the sample to the water that freezes around 0 °C. The difference between these two values is classified as nonfreezing strongly bound water that remains confined around the surfactant polar head groups.

Although the occurrence and description of these phases are well-known and have been reported in several studies,[19,23−30] the real meanings of terms such as gels and intermediate water need to be clarified.

With these premises, we undertook an NMR study to investigate the structure and dynamics at a molecular level of L-ASC12 and D-ASC12 (see Figure 2) in D_2O on the basis of the acquisition and analysis of ^2H- and ^{13}C NMR spectra. NMR characterizations of gel and coagel phases have been reported in the literature, but most of them specifically concerned

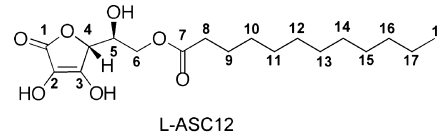

L-ASC12

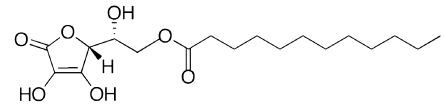

D-ASC12

Figure 2. Molecular structures of L- and D-ASC12.

surfactants different from those here studied and in particular monoglyceride/water systems (see, for instance, refs 29−31).

L-ASC12 and D-ASC12 were dissolved in deuterated water in order to exploit the NMR properties of the deuterium nuclei to gain insights into the structural and dynamic properties of water in the formed gel and coagel phases. Deuterium is a quadrupolar nucleus, with nuclear spin $I = 1$, whose NMR spectrum in anisotropic phases is strongly affected by first-order effects of the quadrupolar interaction, that is, the interaction between its quadrupole moment and the electric field gradient in its environment. In isotropic phases, the quadrupolar interaction is averaged to zero by the fast isotropic tumbling motions of the molecules, while in anisotropic phases it gives rise to peculiar spectral features from which structural and dynamic information on the molecules or molecular fragments bearing the deuterium nuclei can be obtained. The main advantage of using ^2H rather than ^1H NMR consists in the possibility of selectively observing the aqueous fraction and, moreover, of directly interpreting the spectral features in terms of water dynamics because of the purely intramolecular nature of the quadrupolar interaction. Indeed, ^2H NMR has been extensively used in the study of both solids and liquid-crystals.[32−34] In particular, the structural and dynamic properties of water have been characterized through ^2H NMR in ice,[35] lyotropic liquid crystalline phases,[36−38] phospholipid membranes,[39−41] food polymers,[42] and solid organic[43−45] and inorganic hydrates.[46−49] Here, in addition to the ^2H spectral properties, the observation of the ^{13}C nuclei was exploited to investigate the different conformational/dynamic properties of the ASC12 alkylic chains in the gel and coagel phases as well as possible differences between the two diastereoisomers. Ascorbic acid in solution has been already extensively characterized through solution NMR.[50−54] A solid-state NMR study has been reported on some derivatives

TABLE 1: Temperature and ΔH Values for the Coagel-to-Gel Phase Transitions of 60% w/w Dispersions of D-ASC12 and L-ASC12 in H_2O and D_2O from DSC Thermograms

Sample	T (°C)[a]	ΔH (kJ/mol$_{surf}$)
D-ASC12/D_2O	47.1	53.8
D-ASC12/H_2O	45.6	51.5
L-ASC12/D_2O	53.3	48.6
L-ASC12/H_2O	51.5	47.8

[a] Experimental error ±1%. [b] Experimental error ±3%.

of L-ascorbic acid,[55] while to the best of our knowledge, this is the first NMR characterization of the 6-*O*-ascorbyl alkanoates in water.

Experimental Methods

Sample Preparation. Dodecanoyl-6-*O*-D-isoascorbic acid (D-ASC12) and dodecanoyl-6-*O*-L-ascorbic acid (L-ASC12) were synthesized as described elsewhere.[3] Deuterium oxide (99.90% D) was purchased from Euriso-top (Saclay, France).

The samples (L- and D-ASC12/D_2O) were prepared by weighing appropriate amounts of each surfactant and the solvent in order to obtain final compositions of 60 ± 1 w/w%. An annealing procedure was required to obtain homogeneous samples. To make sure that the delicate redox active ascorbic moiety remained intact, the samples were quickly annealed (four heating−cooling cycles around the phase-transition temperature), were stored in a refrigerator at 4 °C, and then were immediately used.

Differential Scanning Calorimetry. DSC runs were acquired with a Q1000 differential scanning calorimeter (TA Instruments) using hermetic aluminum pans. The coagel−gel phase-transition temperature was taken as the temperature of the endothermic peak. The runs were made at the rate of 2 °C/min. For the measurement of the frozen strongly bound water, the samples were first heated to 80 °C, then were cooled to −80 °C, and finally were heated up to 80 °C at 2 °C/min. The enthalpy change of fusion for H_2O is 333.79 J/g and for D_2O is 299.95 J/g.[56]

NMR Experiments. ^{2}H and ^{13}C NMR spectra were acquired on a Varian InfinityPlus 400 spectrometer, equipped with a 5 mm goniometric probe, working at a Larmor frequency of 399.89, 61.38, and 100.57 MHz for ^{1}H, ^{2}H, and ^{13}C, respectively. The 90° pulse length for ^{2}H and ^{13}C was 4.0 μs. ^{2}H spectra were acquired in static conditions by the quadrupole echo pulse sequence ($90°_x-\tau-90°_y-\tau-$acquisition) with τ of 20 μs accumulating 10 000 transients with a recycle delay of 5 s. ^{13}C direct excitation spectra were acquired in static conditions with high-power decoupling from protons using a depth pulse sequence[57] for eliminating probe background signal accumulating 4000 transients with a recycle delay of 10 s. ^{13}C chemical shifts were referred to tetramethylsilane (TMS) as external reference.

^{2}H spectral simulations were performed with WSOLIDS program.[58]

Results and Discussion

Differential Scanning Calorimetry. DSC experiments were performed to detect the phase-transition temperature and enthalpy change for the 60% w/w D-ASC12 and L-ASC12 in H_2O and D_2O. The values are reported in Table 1. The heating−cooling cycles were repeated at least three times. The phase transition is fully reversible. The results indicate that the presence of D_2O increases the phase-transition temperature of about 2 °C with respect to the H_2O dispersion. The phase-transition enthalpy change is always larger for D-ASC12/water than for L-ASC12/water and slightly increases for D-ASC12 when H_2O is replaced by D_2O. Considering that the solvation contribution to the total ΔH (ΔH_{hydr}) is always negative, the data seem to suggest that L-ASC12 is more solvated than D-ASC12 and that H_2O hydrates the D-ASC12 head groups more efficiently than D_2O.

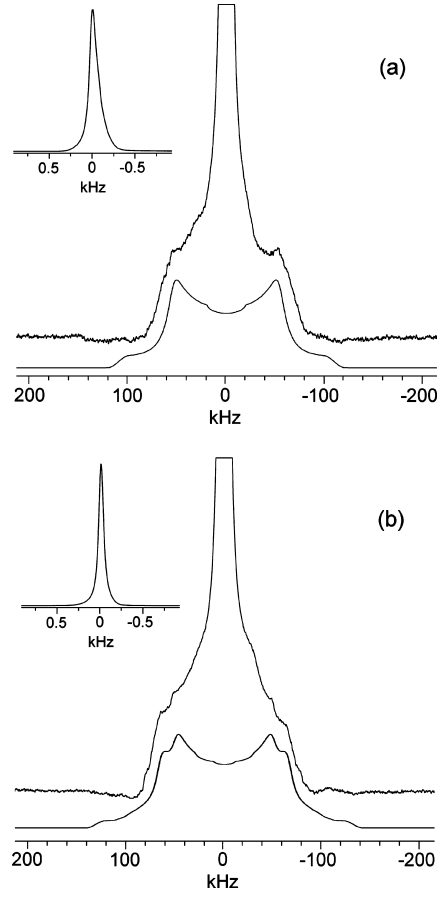

Figure 3. ^{2}H NMR spectra of (a) D-ASC12/D_2O and (b) L-ASC12/D_2O in the coagel phases (25 °C). The upper and lower traces of each figure are the experimental and simulated spectra, respectively. The vertical scale has been expanded in order to optimize the visualization of the broad patterns. The whole narrow peaks are reported in the insets.

^{2}H NMR: Coagel Phases. Figure 3a and 3b shows the ^{2}H NMR spectra of L- and D-ASC12/D_2O in the coagel phases. Both spectra show two different components: a very intense narrow peak (see the insets of the figures) and a broad and less intense pattern centered at approximately the same resonance frequency. The presence of these two components clearly indicates the coexistence of two motionally different kinds of water. The broad patterns are typical of deuterium nuclei in solidlike phases, while the narrow peaks arise from deuterons in isotropic phases.

In an anisotropic phase, because of the absence of fast isotropic tumbling motions, the ^{2}H quadrupolar interaction is not averaged to zero, and the distribution of different orientations of the D_2O molecules with respect to the external magnetic field results in broad patterns. For both samples, a refined spectral simulation of the broad patterns is prevented by the strong overlap with the much more intense narrow peaks, but an approximated simulation can be still attempted. In the case of D-ASC12/D_2O, the observed line shape seems to be well reproduced by a powder pattern of ^{2}H nuclei characterized by

TABLE 2: ^2H NMR Parameters of D- and L-ASC12/D_2O in Coagel and Gel Phases as Determined from Spectral Simulations

Coagel			
Sample	^2H site	χ (kHz)[a]	$I\%$[b]
D-ASC12/D_2O	rigid D_2O[c]	147	100
L-ASC12/D_2O	rigid D_2O-1[d]	175	60
	rigid D_2O-2[d]	132	40
Sample	^2H site	$\Delta\nu$ (Hz)[e]	$G/L\%$[f]
D-ASC12/D_2O	mobile D_2O	120 ± 5	0
L-ASC12/D_2O	mobile D_2O	66 ± 2	0
Gel			
Sample	^2H site	$\Delta\nu$ (Hz)[e]	$G/L\%$[f]
D-ASC12/D_2O	intermediate D_2O	390 ± 5	90
L-ASC12/D_2O	intermediate D_2O	340 ± 5	70

[a] Quadrupole coupling constant. [b] Relative percentage integral. [c] A ^2H asymmetry parameter, η, equal to zero and a Lorentzian line broadening of 15 kHz were used in the spectral simulation. [d] A ^2H asymmetry parameter, η, equal to zero and a Lorentzian line broadening of 12 kHz were used in the spectral simulation. [e] Line width at half-height. [f] Gaussian over Lorentzian shape percentage ratio.

a quadrupole coupling constant $\chi = 147$ kHz assuming an asymmetry parameter $\eta = 0$. χ and η are defined as $\chi = (eQV_{zz})/(h)$ and $\eta = (V_{xx} - V_{yy})/(V_{zz})$, where Q is the ^2H nuclear quadrupole moment and V_{ii}'s are the principal components of the electric field gradient tensor at the observed deuteron ordered in such a way that $|V_{zz}| \geq |V_{yy}| \geq |V_{xx}|$.

The simulation was performed by including a Lorentzian line broadening of 15 kHz that takes into account the intrinsic ^2H spin−spin relaxation time T_2 as well as the distribution of mobility, chemical environment, and hydrogen bond interactions experienced by the water molecules. As often found in static ^2H spectra of solids, the perfect reproduction of the edges of the pattern is prevented by experimental factors like the radiofrequency dishomogeneity. In the case of L-ASC12/D_2O, the observed line shape could be simulated with the combination of two ^2H powder patterns with $\chi = 175$ kHz and $\chi = 132$ kHz, both with $\eta = 0$, with relative weights of 60% and 40%, respectively. Also in this case, a considerable Lorentzian line broadening (12 kHz) had to be included into the spectral simulation. The parameters used in the spectral simulations are summarized in Table 2.

It is known that ^2H nuclei in ice, at sufficiently low temperatures where reorientational motions are completely frozen, are characterized by $\chi = 216$ kHz and $\eta = 0.1$.[35] In the spectral simulations performed on ASC12/D_2O, $\eta = 0$ was assumed for the sake of simplicity, but similarly good simulations could be obtained with $\eta = 0.1$ and slightly different values of χ (by less than 5%). The χ values obtained are clearly smaller than that of ice, although they are still very large. Since ^2H quadrupolar parameters of water are known to be substantially unaffected by differences in chemical environments (similar parameters are indeed found for ice in phospholipid membranes and organic and inorganic hydrates[39,43,45]), the reduced coupling constant values must be interpreted in terms of a partial motional averaging of the quadrupolar interaction. Indeed, ^2H line shapes are very sensitive to molecular motions: in the case of anisotropic phases, when the correlation times of the motions are longer than 10^{-3} s, the solid line shape is not affected. In the range between 10^{-3} and 10^{-7} s, peculiar ^2H line shapes are observed that cannot be fitted with effective first-order quadrupolar parameters. Instead, for faster motions (correlation times shorter than 10^{-7} s), motionally averaged line shapes that can be fitted with reduced effective first-order quadrupolar parameters are obtained.[43,59] The powder patterns of ASC12/D_2O are therefore presumably because of fast, but strongly anisotropic, reorientational motions of the water molecules. Similar shapes were also observed for water in lyotropic liquid crystalline phases and phospholipid membranes and are attributed to anisotropic reorientational motions of water.[39,41] Anyway, the χ values found for ASC12/D_2O coagels are about 2 orders of magnitude larger indicating that the water molecules experience a remarkably lower degree of mobility than in lyotropic liquid crystals and phospholipid membranes and are indeed in a solidlike environment. A rough estimate of the degree of mobility of the fraction of rigid water in ASC12/D_2O with respect to that of motionally frozen water in ice can be obtained by the ratio between the corresponding χ values. In the case of D-ASC12/D_2O, a single powder pattern has been detected with a corresponding motional scaling factor of 0.68 with respect to ice. In the case of L-ASC12/D_2O, two different χ's have been detected suggesting the presence of two motionally slightly different fractions of rigid water with motional scaling factors of 0.81 and 0.61.

The D_2O intense narrow signal (see the insets of Figure 3a and 3b) in L-ASC12/D_2O and D-ASC12/D_2O is well reproduced by a Lorentzian peak with a line width of 66 and 120 Hz, respectively. In both cases, this signal is typical of an isotropic phase, where the quadrupolar interaction is completely averaged out by fast isotropic tumbling motions. However, these signals are broader than those of pure liquid D_2O obtained in the same experimental conditions indicating either a larger heterogeneity of the chemical environment or a slightly more restricted mobility with respect to pure liquid water, which is more considerable in the case of D-ASC12/D_2O.

The presence of two clearly distinguished signals (ascribed to rigid and mobile water) indicates that the exchange between these two water fractions, if present, is very slow. The results here obtained are in very good agreement with the model of the coagel phase. Indeed, it is straightforward to identify the fast isotropically reorienting water with the so-called bulk water and the rigid water with the strongly bound water occupying the thin interlayers between the hydrophilic surfaces of two facing ASC12 lamellae for which the interaction with the ASC12 head groups and the confinement would be responsible for the restricted mobility. Concerning the comparison between the water properties in the coagels of L- and D-ASC12/D_2O, the ^2H NMR results indicate that two slightly different fractions of strongly bound water are present in the case of L-ASC12, while only one has been detected in D-ASC12. Moreover, the bulk water in D-ASC12 seems to be less mobile and seems to be constituted by a larger distribution of molecules experiencing slightly different chemical environments than in L-ASC12.

The integrals of bulk water signals represent approximately 90% of the total area of the ^2H spectra, while those of the strongly bound water constitute the remaining 10%. These integral values are not strictly quantitative, and in particular, those of the powder patterns are likely to be underestimated because of the already mentioned inhomogeneity of the radiofrequency. Moreover, a small contribution to ^2H spectra arising from deuterium nuclei exchanged between water and ASC12 molecules cannot be completely ruled out. On the other hand, in DSC measurements, the strongly bound water is identified as the solvent that does not melt at 0 °C for H_2O and at 3.82 °C for D_2O. The content of strongly bound water estimated from

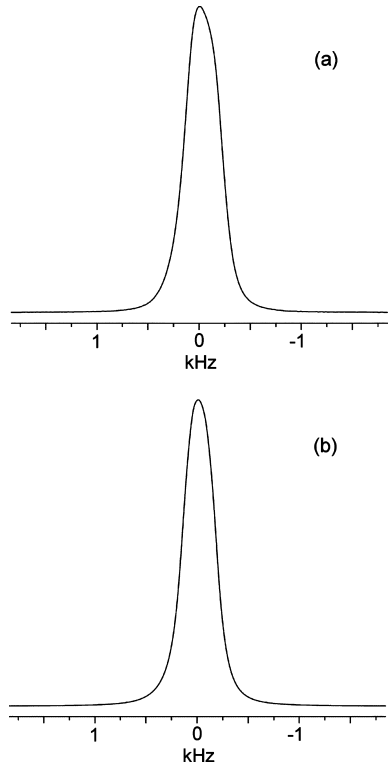

Figure 4. ^{2}H NMR spectra of (a) D-ASC12/D_2O and (b) L-ASC12/D_2O recorded at 52 and 58 °C, respectively, in the gel phase.

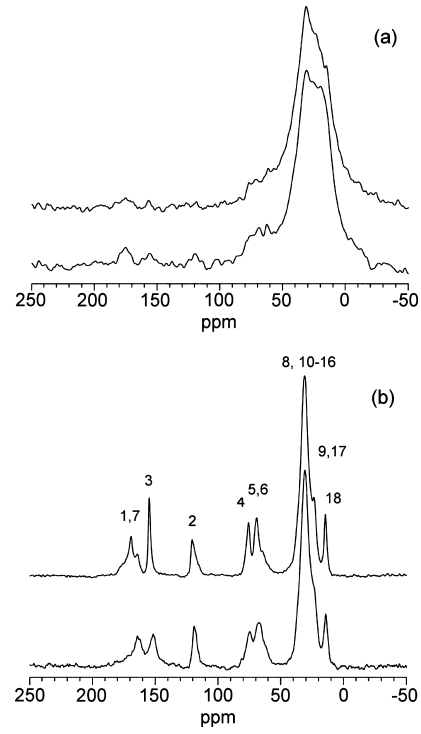

Figure 5. ^{13}C NMR spectra of L- (lower trace) and D-ASC12/D_2O (upper trace) in the (a) coagel (25 °C) and (b) gel (58 and 52 °C, respectively) phases. The signal assignment is reported using the carbon atoms numbering shown in Figure 2.

DSC experiments, for D-ASC12 and L-ASC12 in D_2O and H_2O, ranges between 30 and 35% of the overall amount of water in the sample. However, this calculation of the strongly bound water content is actually an indirect estimation obtained by subtracting from the stoichiometric total amount of water in the sample that of the water that melts at its normal melting point. Therefore, this value is probably overestimated. Furthermore, while the NMR results refer to measurements performed at room temperature, the DSC method to estimate the strongly bound water content refers to the melting point of the pure solvent.

^{2}H NMR: Gel Phases. Figure 4a and 4b shows the ^{2}H NMR spectra of L-ASC12 and D-ASC12/D_2O in the gel phase. The difference with respect to the spectra in the coagel phase is clear. The spectra of both gel phases are composed by just a single peak with line widths of 390 and 340 Hz for D-ASC12 and L-ASC12, respectively. For both samples, the peaks have a mainly Gaussian shape (90 and 70%, respectively, see Table 2). Both signals do not show the typical features arising from the quadrupolar interaction indicating that all the D_2O molecules in the gel phases experience quite fast and isotropic reorientational motions. The Gaussian shape and the larger line width indicate that the average mobility of water in the gel phases is more restricted than that of bulk water in the coagel. This result has a very good correspondence with the model for the gel phase of ASC*n*/D_2O systems (see Figure 1), where the bulk free water disappears and penetrates the interlamellar space, assuming an intermediate mobility between that of the bulk and of the strongly bound water molecules. Moreover, the disappearance of the powder patterns, present in the coagel phases, clearly indicates that also the strongly bound water is no longer detectable in the gel phases and that, therefore, the intermediate water results from the merging of strongly bound and bulk water present in the coagel.

^{13}C NMR: Coagel Phases. Figure 5a reports the ^{13}C NMR spectra of L-ASC12 and D-ASC12/D_2O coagel phases acquired in static conditions with high-power decoupling from protons. For both samples, the lack of spectral resolution is almost complete: only an unresolved broad signal can be observed approximately between −20 and 100 ppm presumably mostly ascribable to the carbon nuclei of the alkylic chains, which are expected to have an isotropic chemical shift of about 30−33 ppm. Other carbon signals are probably too weak and broad to be recognized. This complete lack of resolution is an unambiguous indication that ASC12 molecules in the coagel have a very restricted mobility thus retaining most of the anisotropy of the chemical shielding interaction, which is the main reason for signals broadening. The breadth of the main signal is indeed compatible with the typical ^{13}C chemical shielding tensors of chain methylene carbons in organic solid compounds[60] also considering the overlap with the signals of the terminal methyl and methylene groups. The ^{13}C NMR spectra are in agreement with the X-ray diffraction data of the coagel phases of ASC12/D_2O[61,14] that reflect the significant crystallinity of the system with a lamellar thickness corresponding to the length of ASC12 in its fully stretched conformation and an ordered arrangement of the alkylic chains in orthorhombic or monoclinic packing.

^{13}C NMR: Gel Phases. The ^{13}C NMR spectra of L-ASC12 and D-ASC12/D_2O in the gel phase acquired in static conditions with high-power decoupling from protons are shown in Figure 5b. The coagel-to-gel transition leads to a very good spectral resolution: here, the signals arising from chemically nonequivalent carbons belonging to the polar heads and to the alkyl chains can be distinguished and well identified. This is clear evidence of the activation at the coagel-to-gel transition of motions that strongly reduce the ^{13}C chemical shielding anisotropy (CSA) and thus are characterized by frequencies much larger than 14 kHz (which is approximately the largest CSA arising from the carbonyl groups[60]). The observed signals have an almost isotropic shape but with a line width larger than that of similar

TABLE 3: ^{13}C Chemical Shift (ppm) of D- and L-ASC12/D_2O in the Gel Phase[a]

Carbon Number	1	2	3	4	5	6	7	9	8,10−16	17	18
D-ASC12/D_2O	164.3−176.6	120.9	155.0	76.0	69.4	69.4	164.3−176.6	23.9	31.2	23.9	14.8
L-ASC12/D_2O	164.6	119.4	152.0	75.2	68.9	68.9	164.6	23.6	31.2	23.6	14.6

[a] The experimental uncertainty on the chemical shift values is ±0.2 ppm.

organic molecules in pure liquid phases indicating that the mobility in the gel phases is, however, somehow restricted. The dynamic processes that are activated at the coagel-to-gel transition certainly include the fast trans−gauche interconformational motions of the alkyl chains as revealed by the chain methylene carbon signal resonating at 31.2 ppm. Moreover, the substantially isotropic shape of the peaks indicates the occurrence of some isotropic reorientational motions probably involving the entire lamellar aggregates. Reorientational motions of the alkyl chains within the aggregates are also likely to occur, but they cannot account for the almost isotropic shape of the peaks. These results are different from that previously observed in monoglyceride/water gel phases, where the alkyl chains were characterized by a very restricted mobility (and in particular by the absence of fast trans−gauche interconformational motions) and a hexagonal arrangement.[30,31,29]

The spectra of D-ASC12 and L-ASC12 are very similar, and the peaks can be assigned on the basis of the ^{13}C chemical shift values obtained for pure ascorbic acid in solution[50] and in the solid state[55] as well as from semiempirical calculations (see Figure 5 and Table 3). The experimental chemical shifts are compatible only with the structure reported in Figure 2 ruling out the presence of other tautomeric forms as already reported for pure ascorbic acid in water solution[50] and in the solid state.[62] Moreover, the chemical shifts are very similar to those obtained for pure ascorbic acid in water at pH = 2, when the acid is mainly in its undissociated form. The first deprotonation, occurring at the most acidic site (C_3−OH, pK_a = 3.36 for L-ascorbic acid and 3.29 for D-isoascorbic acid), should cause a strong increase of the chemical shift of C_3 (up to a maximum of 176 ppm) that we did not observe. Indeed, the small ionization of ASC12 is compatible with the strong attracting forces among the long alkyl chains in the aggregates and the favored ion−dipole interactions between RCOOH and RCOO− species which stabilize the charge and disfavor the deprotonation of further carboxylic groups in the aggregates.[17]

Actually, a quite strong difference with respect to the spectra of pure ascorbic acid concerns the signals of carbonyl carbons, which appear as quite broad and structured signals resonating between 160 and 175 ppm, while for pure ascorbic acid a minimum chemical shift of about 174 ppm has been reported for C_1 as a function of pH.[50] On the other hand, the chemical shift of C_7 is also expected to resonate at quite high chemical shift values (around 173 ppm) according to semiempirical calculations. Therefore, the low chemical shifts here observed can only be explained with the small ionization of the ASC12 head groups combined with peculiar chemical environments of carbonyl groups in these phases because of intermolecular and intramolecular interactions as well as hydrogen bonds with solvating water molecules. The broadness of these signals can actually result from the distribution of different chemical environments experienced by carbonyl groups and from a restricted mobility.

The comparison of the spectra of the two samples clearly indicates that all the signals of D-ASC12/D_2O are narrower than the corresponding peaks in L-ASC12/D_2O. This can be ascribed either to a larger average mobility of the gel phase of D-ASC12/D_2O with respect to that of L-ASC12/D_2O or to a larger heterogeneity of the chemical environments experienced by L-ASC12 molecules.

The C_3 signal is the only one showing a significant chemical shift difference (of about 3 ppm) between L-ASC12 and D-ASC12 indicating that the chemical environment experienced by this carbon is different in the two diastereoisomeric systems. Moreover, this carbon shows the largest difference in line width in passing from L to D. This parallels the observation that the D-ASC12 isomer can establish a C_5−C_3 intramolecular hydrogen bond, which is prevented in the L-ASC12 compound because of the different configuration.[17] Also, the carbonyl signals are quite different in the two samples: in L-ASC12, a main peak is observed at 164.3 ppm, while in the case of D-ASC12, the most intense signal is actually at 168.7 ppm. If this signal were assigned to C_1, it would indicate the presence of stronger hydrogen bonds that involve this atom in D-ASC12.[63] Such a conclusion could be in agreement with the existence of significant intramolecular interactions in this diastereoisomer.[17]

Conclusions

The NMR study on L-ASC12 and D-ASC12 in D_2O provided an accurate and extensive investigation of the structural and dynamic properties of the gel and coagel phases formed by these vitamin C-based surfactants. ^2H NMR confirmed the model previously proposed by Kodama and Seki for the coagel-to-gel transition, where the existence of different kinds of water is envisaged. In the coagel phases, two very different water fractions were observed: a prevalent very fast and isotropically moving bulk water and a water experiencing very restricted and anisotropic dynamics, which could be identified with the water confined in the thin aqueous interlayers located between the ASC12 lamellae and that strongly interacts with the surfactant head groups. On the other hand, in the gel phases, only one kind of water was observed experiencing isotropic tumbling motions but showing a more restricted average mobility with respect to coagel bulk water. This latter kind of water, identified as intermediate, is expected to appear in the gel phase as a consequence of the inclusion of the bulk water in thicker interlamellar layers. Moreover, the strongly bound water present in the coagel phase was no longer detectable in the gel one, so that the intermediate water seemed to arise from the merging of strongly bound and bulk water. ^2H NMR parameters such as quadrupolar tensors and line widths were determined for strongly bound, bulk, and intermediate water. The comparison of these parameters with those typical of water in different systems and phases allowed the estimation of an average degree of mobility of water in gel and coagel phases. Some small differences in the dynamic parameters of water were observed between the two diastereoisomers suggesting a possible influence of the different head group configuration on the water arrangement in terms of mobility and interactions. Finally, the ^{13}C spectra unambiguously showed that in the coagel phases surfactant molecules have a very restricted mobility in agreement with the known crystallinity of these mesophases, while the gel phases are characterized by fast trans−gauche interconforma-

tional motions of the alkyl chains and isotropic reorientational motions of the whole aggregates. The comparison between the spectra of D-ASC12 and L-ASC12/D_2O in the gel phases suggested a higher phase mobility and a more homogeneous arrangement of the surfactant molecules in the former. Differences in the signals of C_3 and carbonyl carbons were detected between the two diastereoisomers and seem to suggest the existence of different inter- and intramolecular interactions.

Acknowledgment. The authors acknowledge the Consorzio Interuniversitario per lo Sviluppo dei Sistemi a Grande Interfase (CSGI, Florence) and the Ministero dell'Istruzione, dell'Università e della Ricerca (MIUR, Rome) for partial financial support. Prof. R. Wasylishen is gratefully acknowledged for the helpful discussion and for providing the WSOLIDS program.[58]

References and Notes

(1) Ninham, B. W.; Lo Nostro, P. Molecular Forces and Self Assembly. In *Colloid, Nano Sciences and Biology*; Cambridge University Press: Cambridge, United Kingdom, 2010.
(2) Ambrosi, M.; Fratini, E.; Alfredsson, V.; Ninham, B. W.; Giorgi, R.; Lo Nostro, P.; Baglioni, P. *J. Am. Chem. Soc.* **2006**, *128*, 7209–7214.
(3) Capuzzi, G.; Lo Nostro, P.; Kulkarni, K.; Fernandez, J. E. *Langmuir* **1996**, *12*, 3957–3963.
(4) Capuzzi, G.; Kulkarni, K.; Fernandez, J. E.; Vincieri, F. F.; Lo Nostro, P. *J. Colloid Interface Sci.* **1997**, *186*, 271–279.
(5) Lo Nostro, P.; Capuzzi, G.; Romani, A.; Mulinacci, N. *Langmuir* **2000**, *16*, 1744–1750.
(6) Lo Nostro, P.; Capuzzi, G.; Pinelli, P.; Mulinacci, N.; Romani, A.; Vincieri, F. F. *Colloids Surf., A* **2000**, *167*, 83–93.
(7) Palma, S.; Lo Nostro, P.; Manzo, R.; Allemandi, D. *Eur. J. Pharm. Sci.* **2002**, *16*, 37–43.
(8) Palma, S.; Manzo, R. H.; Allemandi, D.; Fratoni, L.; Lo Nostro, P. *J. Pharm. Sci.* **2002**, *91*, 1810–1816.
(9) Palma, S.; Manzo, R. H.; Allemandi, D.; Fratoni, L.; Lo Nostro, P. *Langmuir* **2002**, *18*, 9219–9224.
(10) Palma, S.; Manzo, R. H.; Allemandi, D.; Fratoni, L.; Lo Nostro, P. *Colloids Surf., A* **2003**, *212*, 163–173.
(11) Lo Nostro, P.; Ninham, B. W.; Fratoni, L.; Palma, S.; Manzo, R. H.; Allemandi, D.; Baglioni, P. *Langmuir* **2003**, *19*, 3222–3228.
(12) Palma, S. D.; Maletto, B.; Lo Nostro, P.; Manzo, R. H.; Pistoresi-Palencia, M. C.; Allemandi, D. A. *Drug Dev. Ind. Pharm.* **2006**, *32*, 821–827.
(13) Palma, S.; Manzo, R.; Lo Nostro, P.; Allemandi, D. *Int. J. Pharm.* **2007**, *345*, 26–34.
(14) Ambrosi, M.; Lo Nostro, P.; Fratoni, L.; Dei, L.; Ninham, B. W.; Palma, S.; Manzo, R. H.; Allemandi, D.; Baglioni, P. *Phys. Chem. Chem. Phys.* **2004**, *6*, 1401–1407.
(15) Lo Nostro, P.; Ninham, B. W.; Ambrosi, M.; Fratoni, L.; Palma, S.; Allemandi, D.; Baglioni, P. *Langmuir* **2003**, *19*, 9583–9591.
(16) Lo Nostro, P.; Ramsch, R.; Fratini, E.; Lagi, M.; Ridi, F.; Carretti, E.; Ambrosi, M.; Ninham, B. W.; Baglioni, P. *J. Phys. Chem. B* **2007**, *111*, 11714–11721.
(17) Ambrosi, M.; Lo Nostro, P.; Fratini, E.; Giustini, L.; Ninham, B. W.; Baglioni, P. *J. Phys. Chem. B* **2009**, *113*, 1404–1412.
(18) Lo Nostro, P.; Ambrosi, A.; Ninham, B. W.; Baglioni, P. *J. Phys. Chem. B* **2009**, *113*, 8324–8331.
(19) Kodama, M.; Seki, S. *Adv. Colloid Interface Sci.* **1991**, *35*, 1–30.
(20) Laughlin, R. G.; Munyon, R. L.; Fu, Y. C.; Fehl, A. J. *J. Phys. Chem.* **1990**, *94*, 2546–2552.
(21) Laughlin, R. G.; Munyon, R. L.; Fu, Y. C.; Emge, T. J. *J. Phys. Chem.* **1991**, *95*, 3852–3856.
(22) Laughlin, R. G.; Munyon, R. L.; Burns, J. L.; Coffindaffer, T. W.; Talmon, Y. *J. Phys. Chem.* **1992**, *96*, 374–383.
(23) Carion-Taravella, B.; Lesieur, S.; Chopineau, J.; Lesieur, P.; Ollivon, M. *Langmuir* **2002**, *18*, 325–335.
(24) Tsuchiya, M.; Tsujii, K.; Maki, K.; Tanaka, T. *J. Phys. Chem.* **1994**, *98*, 6187–6194.
(25) Matsuki, H.; Maruyama, S.; Kaneshina, S. *Colloids Surf., A* **1995**, *97*, 21–26.
(26) Sperline, R. P. *Langmuir* **1997**, *13*, 3715–3726.
(27) Muga, A.; Casal, H. L. *J. Phys. Chem.* **1990**, *94*, 7265–7271.
(28) Boots, J. W. P.; Chupin, V.; Killian, J. A.; Demel, R. A.; de Kruijff, D. B. *Biochim. Biophys. Acta* **2001**, *1510*, 401–413.
(29) Cassin, G.; de Costa, C.; van Duynhoven, J. P. M.; Agterof, W. G. M. *Langmuir* **1998**, *14*, 5757–5763.
(30) Chupin, V.; Boots, J.-W. P.; Killian, J. A.; Demel, R. A.; de Kruijff, B. *Chem. Phys. Lipids* **2001**, *109*, 15–28.
(31) Alberola, C.; Blümich, B.; Emeis, D.; Wittern, K.-P. *Colloids Surf., A* **2006**, *290*, 247–255.
(32) Duer, M. J. *Solid-State NMR Spectroscopy*: Blackwell Publishing: Oxford, U.K., 2002.
(33) Geppi, M.; Borsacchi, S.; Mollica, G.; Veracini, C. A. *Appl. Spectrosc. Rev.* **2009**, *44*, 1–89.
(34) Domenici, V.; Geppi, M.; Veracini, C. A. *Prog. Nucl. Magn. Reson. Spectrosc.* **2007**, *50*, 1–50.
(35) Wittebort, R. J.; Usha, M. G.; Ruben, D. J.; Wemmer, D. E.; Pines, A. *J. Am. Chem. Soc.* **1998**, *110*, 5668–5671.
(36) Lawson, K. D.; Flautt, T. J. *J. Phys. Chem.* **1968**, *72*, 2066–2074.
(37) Blackburn, J. C.; Kilpatrick, P. K. *Langmuir* **1992**, *8*, 1679–1687.
(38) Åman, K.; Håkansson, P.; Westlund, P.-O. *Phys. Chem. Chem. Phys.* **2005**, *7*, 1394–1401.
(39) Lee, D.-K.; Kwon, B. S.; Ramamoorthy, A. *Langmuir* **2008**, *24*, 13598–13604.
(40) Yoon, Y. H.; Pope, J.; Wolfe, J. *Colloids Surf., A* **1997**, *129−130*, 425–434.
(41) Yoon, Y. H.; Pope, J.; Wolfe, J. *Biophys. J.* **1998**, *74*, 1949–1965.
(42) Li, S.; Dickinson, L. C.; Chinachoti, P. *J. Agric. Food Chem.* **1998**, *46*, 62–71.
(43) Vogt, F. G.; Brum, J.; Katrincic, L. M.; Flach, A.; Socha, J. M.; Goodman, R. M.; Curtis Haltiwanger, R. *Cryst. Growth Des.* **2006**, *6*, 2333–2354.
(44) Vogt, F. G.; Dell'Orco, P. C.; Diederich, A. M.; Su, Q.; Wood, J. L.; Zuber, G. E.; Katrincic, L. M.; Mueller, R. L.; Busby, D. J.; DeBrosse, C. W. *J. Pharm. Biomed.* **2006**, *40*, 1080–1088.
(45) Bach-Vergés, M.; Kitchin, S. J.; Harris, K. D. M. *J. Phys. Chem. B* **2001**, *105*, 2699–2706.
(46) Larsson, K.; Tegenfeldt, J.; Hermansson, K. *J. Chem. Soc., Faraday Trans.* **1991**, *87*, 1193–1200.
(47) Scholz, G.; Brehme, S.; König, R.; Heidemann, D.; Kemnitz, E. *J. Phys. Chem. C* **2010**, *114*, 10535–10543.
(48) Benesi, A. J.; Grutzeck, M. W.; O'Hare, B.; Phair, J. W. *J. Phys. Chem. B* **2004**, *108*, 17783–17790.
(49) Takeda, S.; Gotoh, Y.; Maruta, G.; Takahara, S.; Kittaka, S. *Z. Naturforsch.* **2002**, *57a*, 419–424.
(50) Berger, S. *Tetrahedron* **1977**, *33*, 1587–1589.
(51) Ogawa, T.; Uzawa, J.; Matsui, M. *Carbohydr. Res.* **1977**, *59*, C32–C35.
(52) Paukstelis, J. V.; Mueller, D. D.; Seib, P. A.; Lillard, D. W., Jr. *Adv. Chem. Ser.* **1982**, *200*, 125–151.
(53) Ruchmann, A.; Lauterwein, J.; Bäcker, T.; Klessinger, M. *Magn. Reson. Chem.* **1996**, *34*, 116–122.
(54) Stephen Reid, R. *J. Chem. Educ.* **1989**, *66*, 344–345.
(55) Casas, J. S.; Castaño, M. V.; García-Tasende, M. S.; Pérez-Alvarez, T.; Sánchez, A.; Sordo, J. *J. Inorg. Biochem.* **1996**, *61*, 97–108.
(56) Feistel, R.; Wagner, W. *J. Phys. Chem. Ref. Data* **2006**, *35*, 1021–1047.
(57) Cory, D. G.; Ritchey, W. M. *J. Magn. Reson.* **1988**, *80*, 128–132.
(58) Eichele, K.; Wasylishen, R. E. *WSOLIDS NMR Simulation Package*, 2000.
(59) Long, J. R.; Sun, B. Q.; Bowen, A.; Griffin, R. G. *J. Am. Chem. Soc.* **1994**, *116*, 11950–11956.
(60) Duncan, T. M. *Principal components of chemical shift tensors: a compilation*; The Faragut Press: Madison, WI, 1997.
(61) Palma, S.; Manzo, R. H.; Allemandi, D.; Fratoni, L.; Lo Nostro, P. *Langmuir* **2002**, *18*, 9219–9224.
(62) Hvoslef, J. *Acta Crystallogr., B* **1968**, *24*, 23–35.
(63) Geppi, M.; Mollica, G.; Borsacchi, S.; Veracini, C. A. *Appl. Spectrosc. Rev.* **2008**, *43*, 202–302.

JP107324E